Tradeoff-mediated Drought Legacy in Soil Microbiome

Abstract

The profound role of soil microbiomes in completing biogeochemical cycling in the Earth System renders pivotal understanding their responses to drought of increasing frequency and severity towards evaluating drought-mediated biosphere-atmosphere interactions. Though with over a-half century of research on drought impacts on soil microbiomes, drought legacy, a phenomenon of persistence (or memory) of past disturbance that has been increasingly observed in soil microbiomes (and broadly across natural systems) and may largely influence microbiome and ecosystem functioning, is still with a yet unresolved explicit mechanism. Here, using a trait-based microbial systems modelling framework with an explicit intra-cellular metabolic allocation of enzymes vs. osmolytes, we revealed a range of drought legacy scenarios from persistent through transient to no legacy at all depending on drought intensity and microbial dispersal. Emerging from the tradeoffs between enzyme investment and drought tolerance at both the physiological and community level, these legacy scenarios can be coherently organized into a space constrained by Y(Yield)-A(Acquisition)-S(Stress), covering tradeoffs between the three primary life history strategies of microorganisms. Any factor or process that can change the trajectory of a community on this space may alter the property of a drought legacy. This overarching mechanistic insight into soil microbiome drought legacy holds tremendous promise to more accurately quantifying soil microbiome resilience and functioning in organic matter decomposition. Meanwhile, this study inspires us to couple microbiome with vegetation with a holistic ecosystem view by capturing major tradeoff dimensions to evaluate drought-biosphere interactions.

1 Introduction

Drought of increasing severity and frequency both regionally and worldwide is an important environmental change affecting the biosphere (e.g., **Borsa et al. 2014; Berdugo et al. 2020**). The soil microbiome is a key driver of element cycling in the Earth system (e.g., **Falkowski et al. 2008**), so microbial responses are integral for evaluating drought impacts on the biosphere. Still, these responses are omitted or implicitly treated in global assessments of drought-biosphere interactions (e.g., **Green et al. 2019**).

Over a-half century of research has uncovered a myriad of physio-chemical, physiological, and ecological mechanisms underlying microbial functional responses to drought disturbance in soil environment (e.g., **Birch 1958; Schimel 2007; Manzoni et al. 2012**). However, increasing studies have suggested that drought may have lasting effects on the soil microbiome and its functioning, even after drought conditions have ended (e.g., **Evans and Wallenstein 2012**; **Meisner et al. 2015**; **Hawkes et al. 2017; Martiny et al. 2017; Hinojosa et al. 2019**). This phenomenon, here termed drought legacy, has also been observed across the forest biome and beyond (e.g., **Cuddington 2011; Anderegg et al. 2015; Johnstone et al. 2016; Conradi et al. 2020**). Still, the mechanistic basis for microbiome drought legacies remains unclear. Such a lack of mechanistic insights hinders a systematic evaluation of drought-ecosystems interactions.

Legacies likely originate from microbiome changes that persist after a drought disturbance. Microbiomes are complex adaptive systems, with their functioning emerging from both individual variations and within-community interactions. Past lab- and field-based efforts explained soil microbiome drought legacies by depicting compositional differences in terms of microbial functional groups with different life-history strategies. Notably, **Hawkes and Keitt (2015)** proposed a mechanism of community shift in relative abundance of moisture generalists vs.

specialists, where generalists are functionally more stable than specialists with variations in moisture. This idea was proposed to explain a lack of change in moisture response across sites in Texas, USA, because of observed dominance by generalist taxa resulting from high variability in historical rainfall (**Hawkes et al. 2017; Waring and Hawkes 2018**). Similarly, **Evans and Wallenstein** (**2014**) argued soils with relatively stable moisture history had more moisture-sensitive taxa and hence larger changes in biomass and composition (**Evans and Wallenstein 2012**).

This pioneering coarse functional group-based depiction of complex microbiomes presents a gap of explicit underlying physiological basis. Physiologically, it is well established that a microbial cell can direct available resources from producing exoenzymes to acquire resources to produce compounds, e.g., osmolytes, to combat desiccation (e.g., **Schimel 2007**), an intra-cellular metabolic plasticity that displays large inter-cellular variability (e.g., **Manzoni et al. 2012**). A missing of the physiological basis cannot tell how a microbial community can be shaped by drought disturbance from physiological interception and community organization and thus how its functional changes can persist. This deficiency becomes especially apparent when having many studies at different sites with varying confounding factors reporting legacies of varying magnitudes with differing time frames, especially those that even did not observe a drought legacy at all (e.g., **Rousk et al. 2013; Fuchslueger et al. 2016**). A similar lack of mechanistic understanding also applies to warming-induced legacies in microbiome functioning (e.g., **Karhu et al. 2014**). We need to link individual-level physiological variations to community-level shifts to explain persistence of microbial functioning.

Trait-based quantification of ecological complexity can bridge the gap between community dynamics and underlying large physiological variability, which would help unravel mechanisms

underlying drought legacy. Trait-based community dynamics and ecosystem functioning has long been established in plant communities (e.g., **McGill et al. 2006**). In soil microbiomes, by quantifying the individual-level metabolic variation using physiological traits that reflect and determine demographic variation between individual cells **Malik et al. (2019)** proposed a trait-based framework, Y-A-S (Yield-Acquisition-Stress), covering tradeoffs between the three primary life history strategies of microorganisms. In addition, a manipulative experiment in a grassland ecosystem in Southern California attributed a drought legacy in litter decomposition to bacterial composition change with an alteration of carbohydrate degradation traits (**Martiny et al. 2017**). This study directly shows the potential to establish trait-based linkages between microbial physiology and community shifts underlying legacies.

Based on the trait-based Y-A-S framework, against the need to increase community-level drought tolerance to combat drought pressure tradeoff-mediated physiological adaptation and turnover of individuals comprising a microbial community should drive a community to lower its enzyme investment. Thereby, a drought legacy in organic matter decomposition may arise from the persistence of this functional change in terms of enzyme investment. With this reasoning, factors that can shift microbiomes along the tradeoff between enzyme investment and drought tolerance could alter the magnitude and duration of drought legacies. For instance, the intensity of drought, which directly modulates intracellular metabolic allocation of enzyme vs. osmolyte (e.g., **Csonka 1989; Schimel 2007**), may strongly drive the position changes along the tradeoff and hence affect the legacy. In addition, dispersal of microbes, a pivotal process influencing community composition and dynamics via introducing taxa (e.g., **Fukami 2015; Vila et al. 2019**), may change the drought-induced position moves along the tradeoff and hence alter drought legacy

92 (**Hawkes et al. 2017**). Therefore, trait-based tradeoffs between drought tolerance and enzyme
93 investment underlying the YAS are hypothesized to govern drought legacies in soil microbiomes.
94 Theory-driven trait-based modelling is well positioned to complement the current
95 generation of lab- and field-based investigations to test trait-based mechanisms underpinning soil
96 microbiome drought legacies. Trait-based modelling in an individual-based framework is able to
97 bridge across scales from individual cells through communities to the ecosystem level by explicitly
98 simulating intra-cellular metabolic processes, ecological dynamics of microbial communities, and
99 emergent functioning (**Allison 2012**). Such a modelling approach can overcome some of the
100 limitations of aggregated modelling approaches that treat microbes as a single biomass pool or a
101 few discrete functional groups [see a review by **Wieder et al. (2015**)]. In addition, testing the claim
102 that including legacy would be trivial in biogeochemical modelling (**Rousk et al. 2013**) offers a
103 direct stimulus for conducting legacy modelling.
104 The goal of our study was to analyze the trait-based, tradeoff-mediated mechanisms
105 underpinning soil microbiome drought legacies. Our approach applied a mechanistically and
106 spatially explicit trait- and individual-based soil microbial systems modelling framework—
107 DEMENTpy, that represents tradeoffs among resource acquisition and drought tolerance at the
108 physiological level and the emergent at the community level. Specifically, we asked the following
109 questions: 1) How does the magnitude of drought legacy in decomposition vary with drought
110 intensity? 2) How does dispersal of microbes affect the formation of drought legacy? 3) What are
111 the underlying changes in traits of enzyme investment and drought tolerance? And 4) can these
112 changes be put into a coherent mechanistic framework based on YAS? We tackled these questions
113 by applying DEMENTpy to a grassland ecosystem in Southern California. Our study exemplifies

how trait-based investigations into microbiome legacies can improve mechanistic understanding of microbial controls on elements' cycling underlying biosphere-atmosphere interactions.

2 Methods

2.1 Model description

DEMENTpy (DEcomposition Model of ENzymatic Traits in Python; GitHub Repository: https://github.com/bioatmosphere/DEMENTpy) is a spatially and mechanistically explicit trait- and individual-based microbial systems modelling framework built upon its predecessor DEMENT (**Allison 2012; Allison and Goulden 2017; Wang and Allison 2019**). This model randomly initializes a microbial community on a spatial grid based on physiological traits and simulates its dynamics by explicitly modelling demographic processes of cell metabolism and growth, mortality, and reproduction for each population at a daily time step. Driven by temperature and moisture, the community secretes different exoenzymes decomposing different organic compounds. Starting from continuous physiological traits, DEMENTpy bridges across scales from individual through community to systems in soil microbiome (see **Supporting Fig. 1** for model structure). Only community initialization and intra-cellular metabolic allocation are highlighted below. More details with respect to structure, processes, formulae, and parameters are included in the **Supporting Information.**

With a trait-based approach, DEMENTpy creates a microbial community composed of a large number of hypothetical taxa by randomly drawing values from uniform distributions of microbial traits and assigning them to different taxa (see a list of traits in **Supporting Fig. 1B** and more details in **Supporting Text**). The traits include rates of enzyme production (constitutive and inducible) and rates of osmolyte production (constitutive and inducible). Drought tolerance of each

taxon is determined by normalizing the inducible osmolyte rate of production to a value from 0 to 1. This formulation establishes a mechanistic connection between osmolyte production and drought tolerance (**Schimel 2007**) in contrast to the previous model version which instead directly introduced a drought tolerance parameter and imposed a penalty on carbon use efficiency accordingly (**Allison and Goulden 2017**).

DEMENTpy explicitly treats intra-cellular metabolism of ingested monomer carbon derived from explicit exoenzymatic degradation of substrates (**Supporting Fig. 1C**; see **Supporting Text** for substrate degradation and other demographic processes). The metabolic processing of assimilated carbon after growth respiration is directed to produce enzyme (and maintenance respiration) and osmolyte (and maintenance respiration), which are treated as simultaneous processes without prescribing an order. After accounting for the constitutive production of enzymes and osmolytes, the carbon left after these inducible processes accumulates toward biomass (denoted as yield). We assume the constitutive osmolyte production rate varies across taxa but independent of water potential, accounting for bacterial/fungal cell's allocation of biomass to keep a water potential balance across the cell wall (e.g., **Csonka 1989; Potts 1994**). By contrast, inducible production of osmolytes is subject to constraints from water potential only below a certain threshold. Mortality of microbial cells is simulated both deterministically by accounting for mass balance and stochastically based on death probability constrained by drought tolerance and water potential.

2.2 Modelling experiments

We applied DEMENTpy to the grassland system at Loma Ridge, Southern California (**Allison et al. 2013**) and parameterized the model with 100 different hypothetical bacterial taxa on a 100 by 100 spatial grid with decomposing grass litter containing ten different substrates (see

parameter values in **Supporting Table 1** and substrates in **Supporting Table 2**). DEMENTpy was benchmarked with the daily weather data of year 2011, which is treated as the ambient scenario (**Supporting Fig. 2A)**, based on which results presented below were robust to reasonably varying the parameter value range of basal enzyme and osmolyte production rate.

In addition to this ambient scenario, we conducted simulations with manipulated drought to examine drought disturbance to the microbial system with respect to responses and recoveries in three 3 phases (**Supporting Fig. 2**). Two drought scenarios, moderate and severe, were created by reducing the water potential across only the dry season by a factor of four and ten, respectively. After the community establishment phase and a successive drought period, the ambient scenario was re-imposed to examine changes in microbial communities degrading substrates. One set of such simulations without dispersal is referred to as default mode. Another set in dispersal mode with only the ambient and severe drought scenario was run to further examine how dispersal affects drought disturbance response over time.

2.3 Simulation protocol and data analysis

With the model setup as above, we conducted three-phase simulations following the protocol as follows (**Supporting Fig. 2**). After establishing an initial microbial community from a randomly constructed microbial pool on the spatial grid with homogeneously distributed substrates, each simulation was run for 10 years at a daily time step (spin-up: 3 years; disturbance: 3 years; recovery: 4 years). Substrates, monomers, and enzymes were reinitialized uniformly on the spatial grid at the start of each new year to have the same concentrations as the very first year except for the microbial community. In each new year, the microbial community on the spatial grid was also randomly reinitialized with the same microbial biomass pool size. Two different methods were applied to differentiate between the default and dispersal mode: for the default mode,

183 microbial community composition was determined according to the biomass frequency of each
184 taxon on the last day of the previous year (**Supporting Fig. 2C**); in dispersal mode, the taxon
185 frequencies were based on the cumulative biomass of each taxon across the entire previous year
186 (**Supporting Fig. 2D**). In contrast to the default mode, the dispersal mode allows taxa dead in a
187 previous year to have a chance to be re-introduced into the community at the start of the next year,
188 accounting for the dispersal bacteria that survive in refugia or that are blown in from nearby wetter
189 areas. These simulations were repeated for each scenario under the two modes (default and
190 dispersal) for 40 times with 40 different random number generation seeds ($5 \times 40 = 200$ runs in
191 total). This sample size was determined by a convergence analysis of DEMENTpy's stochastic
192 nature (**Supporting Fig. 3**).

193 **2.4 Data analysis**

194 All results presented in this work, unless indicated otherwise, were analyses of the
195 ensemble of 40 runs for each of the five scenarios. A dataset was established from these
196 simulations encompassing taxon traits (enzyme investment and drought tolerance), time-series of
197 taxon-specific allocation to enzymes (inducible plus constitutive), osmolytes (inducible plus
198 constitutive), yield, and biomass in carbon, and time-series of compound-specific and total
199 substrates. Taxon-specific allocation to enzymes, osmolytes, and yield were aggregated to derive
200 the corresponding community-level allocation. With taxon traits and biomass, biomass-weighted
201 community-level traits, enzyme investment and drought tolerance, were calculated (see the
202 **Supporting Text** for calculation method). Because the system largely stabilized in 3 years
203 (**Supporting Fig. 2**), results up to year 9 (3rd year of recovery from drought disturbance) are
204 presented. In addition, 95% confidence intervals were presented in most of the cases except for

205 microbial community composition and community carbon allocation, for which results of only one
206 out of the 40 simulations were shown.
207

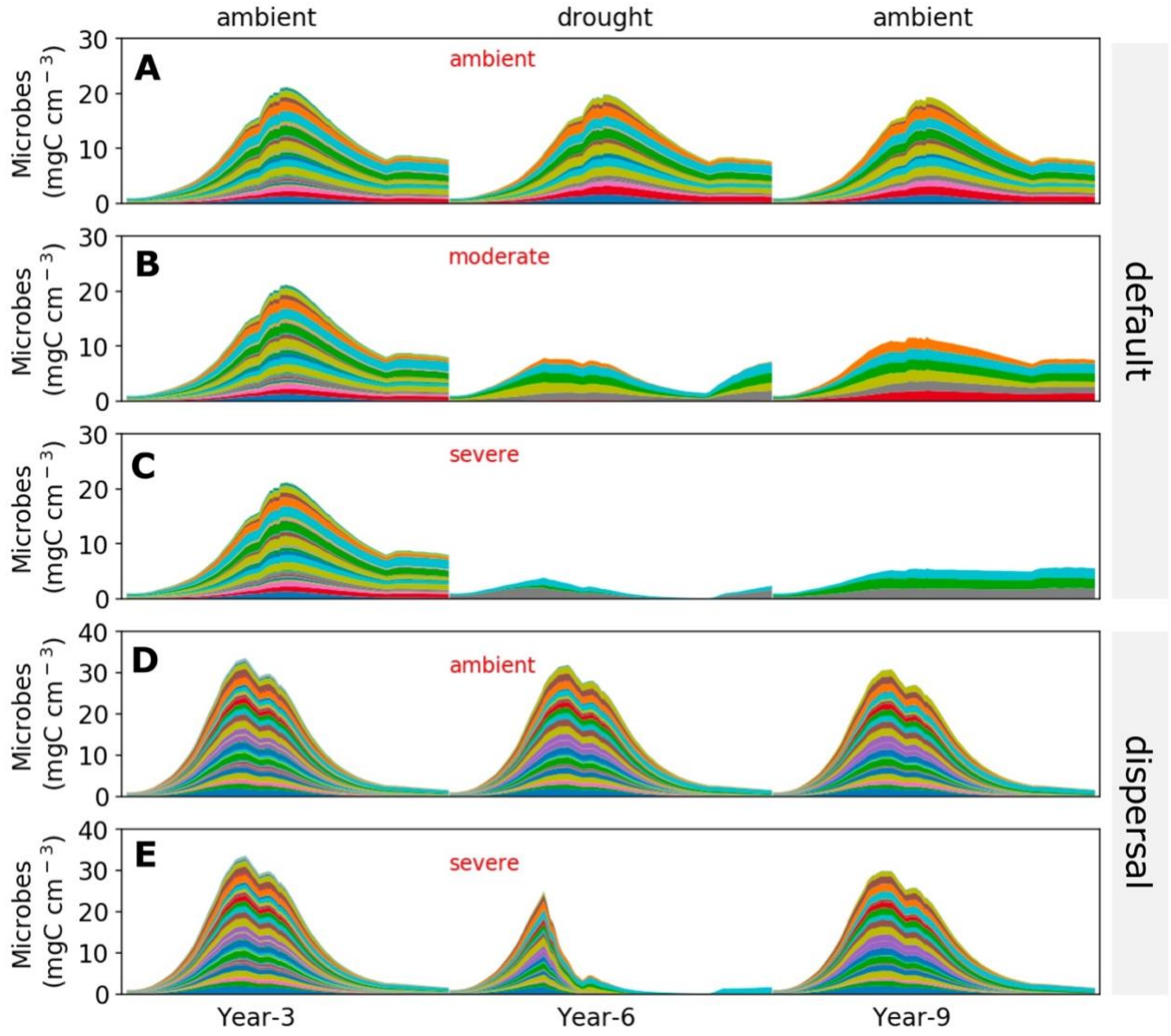

208

209 **Fig.1. Microbial community dynamics disturbed by drought of differing severities with and**
210 **without dispersal.** (**A-C**) Dynamics without dispersal under ambient, moderate, and severe
211 scenario, respectively. (**D, E**) Dynamics with dispersal under ambient and severe scenario,
212 respectively. Colored bands represent different hypothetical taxa in terms of biomass (mg C cm^{-3})
213 averaged over the 100×100 spatial grid. Data shown are only for years 3, 6 (the 3rd year under

drought), and 9 (the 3rd year after drought). See **Supporting Fig. 2** for the full 10-year dynamics under the ambient scenario of both default and dispersal mode.

3 Results

3.1 Microbial community dynamics under the ambient drought scenario

The system became relatively stable after 2 years, with seasonal dynamics in the microbial community repeating across years (**Supporting Fig. 2**). Seasonal dynamics with respect to community composition and biomass reflected a joint control by environment and substrates. Starting from the wet season that was replete with substrates, a microbial community consisting of different taxa established and grew in biomass. As substrates were degraded and depleted, microbial cells began to starve and die. Increasing drought while entering the dry season induced more death. These two processes in combination resulted in the decline of microbial biomass after a biomass peak around 20 mg C cm^{-3} (**Fig. 1A)** and drove the composition toward taxa with higher drought tolerance and lower enzyme investment (**Supporting Fig. 4A**) and hence community level enzyme investment decreased (**Fig. 2A**) and drought tolerance increased across the dry season (**Fig. 2B**). Similar seasonal and inter-annual dynamics were observed for the community with dispersal but with much higher biomass (peaked around 30 mg C cm^{-3}) and taxonomic diversity (**Fig. 1D; Supporting Fig. 4B; Fig. 2C, D**).

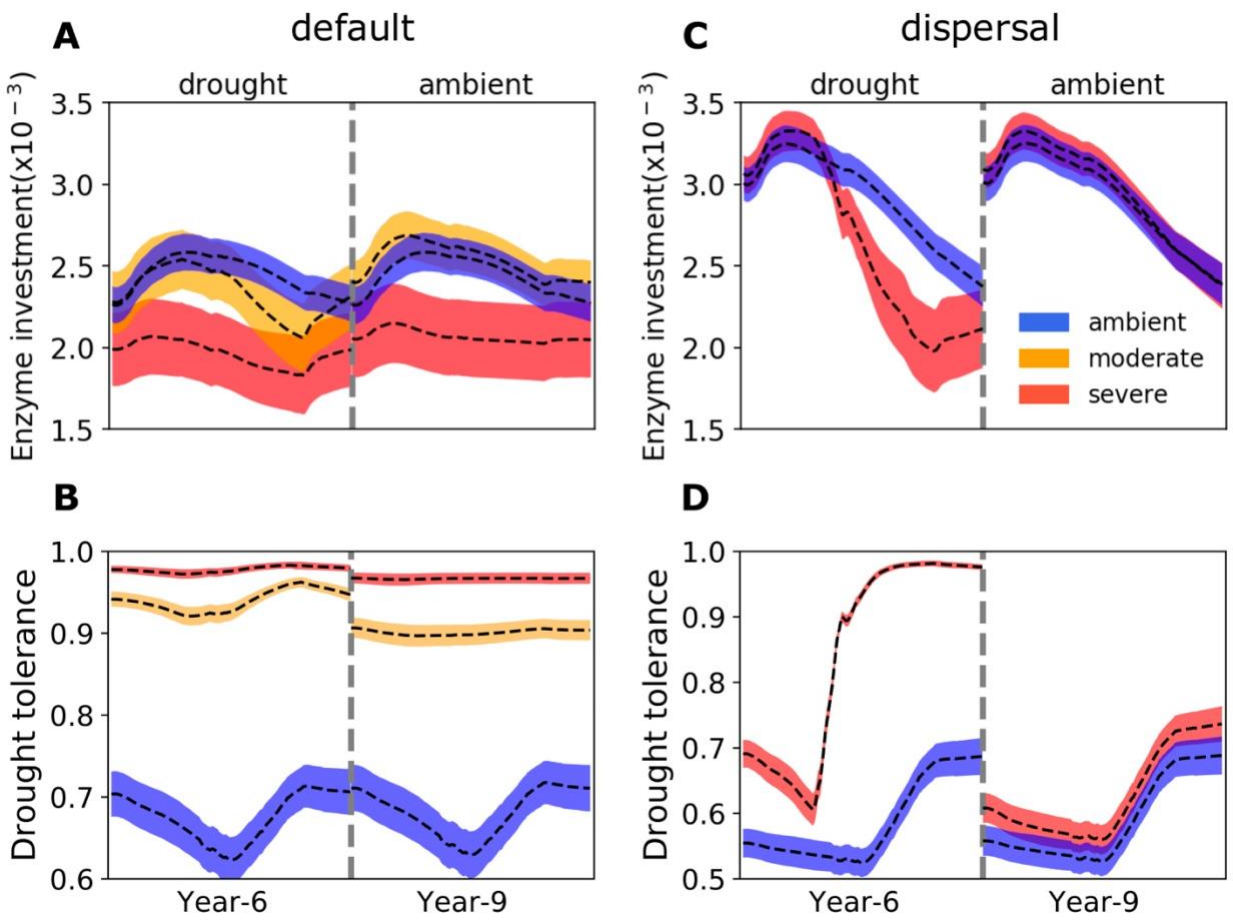

232

233 **Fig.2 Seasonal dynamics of community-level enzyme investment and drought tolerance of**

234 **microbial communities under different drought scenarios.** (**A, B**) Enzyme investment and

235 drought tolerance during year 6 (3rd year under drought) and year 9 (3rd year after drought) under

236 three scenarios (ambient, moderate, and severe) without dispersal, respectively. (**C, D**) The same

237 for communities with dispersal under two scenarios (ambient and severe). Dashed lines and color

238 bands are means and 95% confidence intervals (n=40).

239

240 **3.2 Responses to and recoveries from drought disturbance of varying severity**

241 Variation in drought severity altered the microbial community to varying extents (**Fig. 1B,**

242 **C**). Total biomass declined significantly, with the severe scenario declining the most by about 50%

to a peak less than 10 mg C cm^{-3}. Composition of the communities changed dramatically in terms of taxonomic richness and abundance after 2 years of drought perturbation with differing levels of drought tolerance and enzyme investment. Compared to the ambient scenario, drought tolerance increased significantly across the whole season from as low as only 0.62 to 0.92 of the moderate scenario and to 0.97 of the severe (**Fig. 2A,B**). However, the community enzyme investment only declined significantly in the severe scenario across the dry season and did not change much in the moderate scenario on average besides the later stage in dry season (**Fig. 2A,B**). These trait changes dictated differences in community-level carbon allocation between enzymes and osmolytes and thus yield (**Fig. 3A; Supporting Fig. 5A**). Under the moderate scenario, the percentage of assimilated carbon allocated to osmolytes ranged between 65–85%, compared to the ambient range of 50–70%, whereas enzyme allocation was consistently lower (10% on average) than the ambient (20% on average). However, the resulting yield was basically similar, ranging between 0 - 30%, though a few points in the ambient were higher (reaching at most 40%) early in the drought season. Under the severe scenario, the percentage of osmolytes became even higher and enzymes even lower, and the community yield approached zero more often. Eventually, these differences in community resource allocation between osmolytes and enzymes were manifested in the dampened degradation of substrates over the grid, with the two drought scenarios resulting in different levels of decomposition declines (average of 57.39 and 85.65%, respectively; **Fig. 4A, B**).

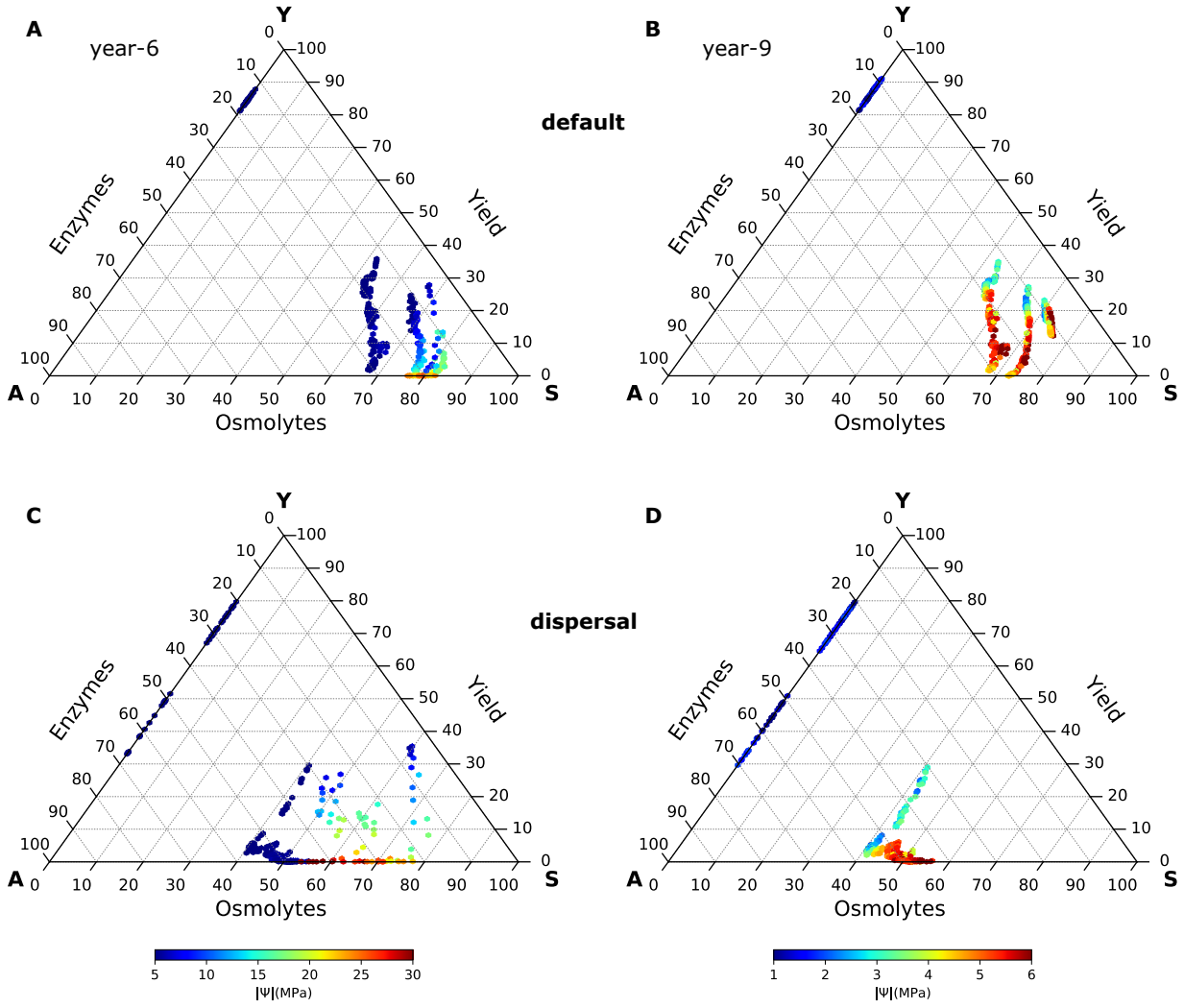

263

264 **Fig. 3 Ternary plots of community-level allocation of assimilated carbon among enzymes,**
265 **osmolytes, and yield over time under different drought scenarios. (A, B**) Enzyme-Osmolyte-
266 Yield tradeoff of communities during year 6 (3rd year under drought) and year 9 (3rd year after
267 drought), respectively, of the default mode (without dispersal). (**C, D**) The same for the dispersal
268 mode. The Y (Yield), A (Acquisition), and S (Stress) labeled at corners correspond to yield,
269 enzymes, and osmolytes, respectively. See **Supporting Fig. 5** for a version with points
270 differentiated by drought scenario instead of water potential.

271

Once the ambient conditions were re-imposed, after 2 years (i.e., year 9) new stable microbial communities formed (**Fig. 1B, C** and **Supporting Fig. 2C**). Compared to the ambient scenario, these newly-formed communities had different drought tolerance and enzyme investment (**Fig. 2A, B**). Drought tolerance was significantly higher under both the moderate (0.90) and severe scenario (0.96) than under the ambient, though both became a little lower than the communities realized under drought disturbance. In contrast, enzyme investment under the moderate scenario became similar to the ambient community, with only the severe scenario community remaining significantly different. Only the severe community showed a clearly lower allocation to enzymes than the ambient community across the dry season (**Fig. 3B; Supporting Fig. 5B**). This loss of differences in enzyme investment in the moderate community eventually resulted in only the severe scenario displaying significantly reduced degradation compared to the ambient scenario (by 47.72% on average; **Fig. 4B**), although the magnitude of decline was dampened compared to the antecedent drought period because of the relief of drought pressure (**Fig. 4A**). It is noteworthy that prior to year 9, the degradation changes resulting from the transient communities (year 7) were significant for both drought scenarios (an average decline by 18.00 and 55.52%, respectively).

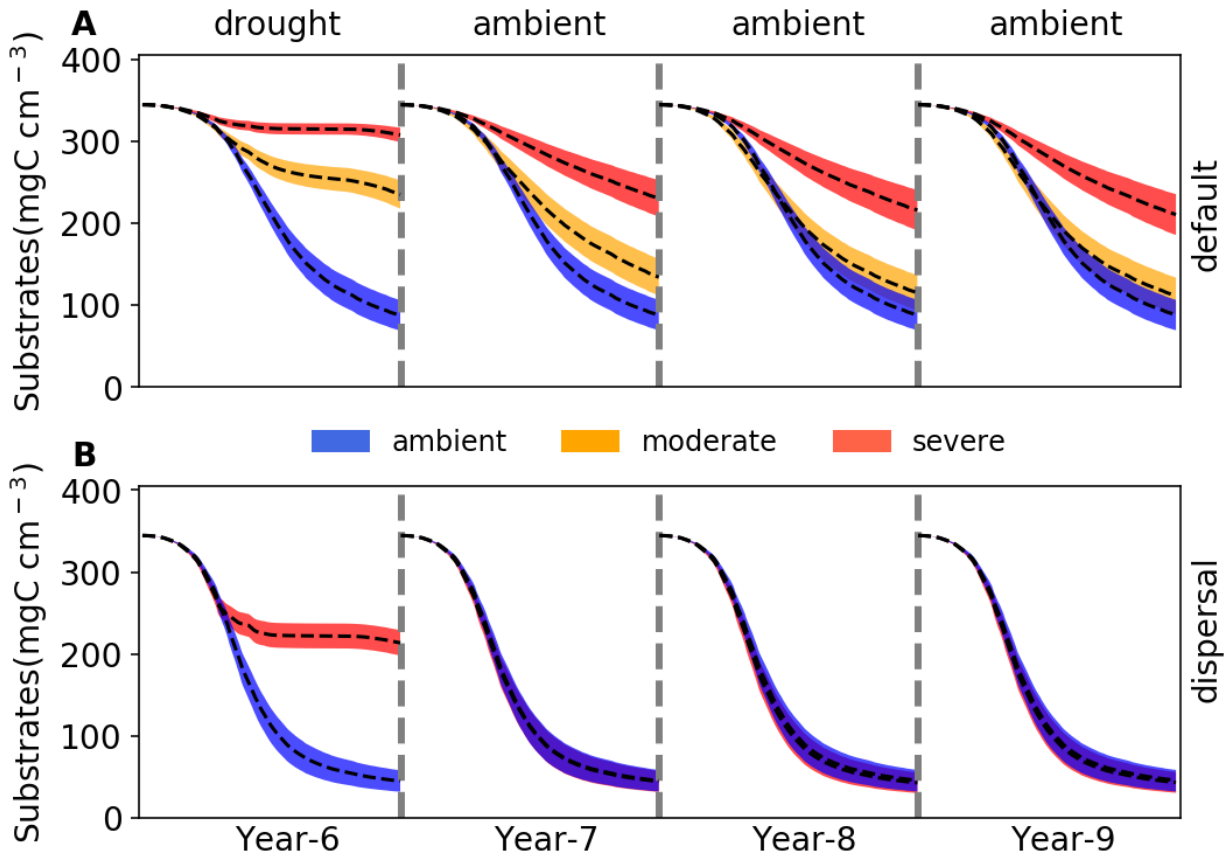

Fig. 4 Changes in substrates driven by drought. (**A**) Total substrates on the spatial grid over year 6-9 under three different scenarios (ambient, moderate, and severe) without dispersal. (**B**) The same for simulations with dispersal under ambient and severe scenarios. Dashed lines and colored bands are means and 95% confidence intervals (n = 40), respectively. See **Supporting Fig. 6** for an example illustration of the underlying substrate-specific changes.

3.3 Responses to and recoveries from the severe drought disturbance with dispersal

With dispersal of taxa from the same microbial pool at the start of each year, the overall responses to the severe drought disturbance were similar to the default mode, though with differing magnitudes and seasonal patterns. With dispersal the microbial community also saw both lower total biomass and declined taxonomic abundance, particularly significant during the dry season,

but remained higher than the default mode (**Fig. 1E**). This stable community realized had significantly different community enzyme investment and drought tolerance from the ambient as well but with a different seasonal pattern compared to the default mode. The enzyme investment sharply declined from a peak of 0.0033 to 0.0020, and the drought tolerance increased sharply from 0.60 to 0.97 across the dry season, increasing their differences from the ambient over time (**Fig. 2C,D**). These changes resulted in the community allocating more assimilated carbon to produce osmolytes and less to enzymes, which resulted in zero yield when drought was most severe during the dry season (**Fig. 3C; Supporting Fig. 5C**). All these changes pointed to significant declines in decomposition of substrates (**Fig. 4C**; an average decline of 56.29% that was lower than the default mode).

However, when ambient conditions were re-imposed, recovery from drought was rapid compared to the default mode. After 2 years, the community became similar to the ambient (**Fig. 1E**), a stark contrast to the default mode (**Fig. 1C**). This compositional similarity coincided with similar community enzyme investment (**Fig. 2C**) and drought tolerance (**Fig. 2D**), which resulted in the same community-level allocation of assimilated carbon among enzymes (30 - 60%), osmolytes (40 - 60%), and thus yield (0 - 30%; **Fig. 3D; Supporting Fig. 5D**). These communities eventually had the almost exactly the same composition and substrates decomposition rates (**Fig. 4D**). In fact, in contrast to the default mode, the transient community did not show significant effects after the 1st year following drought (year 7; **Fig. 4D**). Based on this lack of legacy effects under the severe scenario, we did not find it informative to run simulations of the moderate scenario with dispersal.

4 Discussion

With trait-based modelling in a mechanistically explicit fashion, this study examined the relationships between drought legacy and drought severity and dispersal in simulated litter microbiomes. Manifestation of drought legacy at the system level in terms of litter decomposition was contingent on drought severity and microbial dispersal, ranging from persistent through transient to no legacy at all (**Fig. 4**). Such a set of representative legacy scenarios varying in magnitude and duration emerged from an overarching mechanistic basis—tradeoffs between enzyme production and drought tolerance, which can be coherently organized into a YAS-based framework. Elucidating soil microbiome drought legacies contributes to understanding microbial systems resilience; weaker legacies correspond to higher resilience of soil microbiome functioning in response to historical drought conditions. Our quantification of legacy mechanisms underlying microbial system resilience will help more accurately quantify organic matter decomposition and feedbacks of whole ecosystems to drought in the Earth system.

Transient legacy under moderate drought

Clearly, the severity of drought disturbance influences the magnitude and duration of legacy by determining the extent to which a microbial community can adapt (**Fig. 4A**). Our drought disturbance lasted long enough for communities to reach a stable state. However, our simulations represent only a subset of the broad spectrum of actual drought disturbance in terms of frequency, intensity, and duration and were implemented to uncover and demonstrate the underlying mechanisms. By increasing the drought intensity, we revealed legacies from transient to persistent. Weaker disturbances than we analyzed might result in no legacy at all.

Drought disturbance of a relatively low severity had a negative effect on decomposition conferred by the transient community, but eventually the legacy effect disappeared (**Fig. 4A**), a pattern that we dub "transient legacy". This transient legacy matches the rainfall manipulation experiment with a reciprocal design at our field site, which observed resilience to drought in terms of litter decomposition within three years (**Martiny et al. 2017**). It is noteworthy that our modeled transient legacy arose from a community with the same functioning but different composition and biomass. However, with a total biomass difference as large as 50% at the peak but a similar at the end (**Fig. 1B**), the role of biomass difference in this eventual functional indifference can be largely excluded. This exclusion of biomass change in contributing to legacy formation is consistent with findings from our field experiment (**Martiny et al. 2017**) and a reciprocal transplant study across a climate gradient in Southern California (**Glassman et al. 2018)**. Rather, the eventual loss of legacy fundamentally resulted from the same community enzyme investment though with a different composition (accompanied by a realization of higher community drought tolerance; **Fig. 2A,B**). Such a compositional but not functional change in the eventual new stable system after a disturbance, which has been widely observed across natural systems (e.g., **Ives & Carpenter 2007; Fukami 2015**), reflects a broad notion of functional similarity in the soil microbiome (**Allison and Martiny 2008**). It is this transient legacy that dictates the resilience of microbial systems and other natural systems when moderately perturbed, underlying which functional redundancy is one key factor for microbial systems in particular (e.g., **Louca et al. 2018**).

Persistent legacy under severe drought

In contrast, a persistent legacy can result from a stronger drought disturbance (**Fig. 4B**) that pushes the community to reach an even higher drought tolerance by sacrificing more of the

investment in enzyme production (including a loss of relatively more drought-intolerant taxa), thereby forming a community not only compositionally but also functionally different (**Fig. 2A,B**). A similar long-term legacy in soil heterotrophic respiration was also observed by microcosm and field transplant experiments (**Hawkes et al. 2017)**. This persistent legacy embodies the broad notion of alternative stable state with different functioning in ecological systems. Similar disturbance-contingent alternative stable system has been widely reported across natural systems with disturbances of drought and beyond: e.g., in gut microbiota experiencing transient osmotic perturbation (**Tropini et al. 2018**) and in forest biomes across the tropical (e.g., **Staver et al. 2011**) and the boreal forest (**Herzschuh 2020**), as well as in small pond systems (**Chase 2003**). Intuitively, a persistent legacy means the loss of system resilience with severe disturbance.

Disappearance of legacy under severe drought with dispersal

However, dispersal can negate formation of even a transient legacy in organic matter decomposition (**Fig. 4B**). By introducing taxa from the same microbial pool in each new year, we found that dispersal with even the severe drought disturbance can rescue dead taxa and completely mitigate the physiological tradeoff-mediated drought selection on a microbial community (**Fig. 1E**). As a result of preserving community drought tolerance and enzyme investment (**Fig. 2C,D; Fig. 3D**), dispersal can overwhelm the drought legacy in organic matter decomposition (**Fig. 4B**). This disappearance of legacy suggests that dispersal can increase microbial systems resilience to drought disturbance (**Allison and Martiny 2008**), forming a stark contrast to the persistent legacy induced by the severe drought disturbance without dispersal as discussed above (**Fig. 4B**). We must acknowledge that factors in dispersal influencing resident community are manifold. For instance, timing (e.g., priority effects; **Fukami 2015**) and velocity (e.g., **Evans et al. 2020**) both

have been suggested to be important. In addition, even an unsuccessful invasion by a single dispersal species with only short-term interactions with the resident community can induce an alternative stable state functioning differently (**Amor et al. 2020**). Responding to these variations in the dispersal process, a microbial community could instead present compositional and functional changes to varying extents (e.g., **Fukami 2015**) and hence varying magnitudes of legacy in decomposition. For example, in a field transplant experiment but with passive dispersal Hawkes et al. (2017) did not find apparent mitigation of historical rainfall legacy in soil respiration. Therefore, the treatment of dispersal in this study (with a sole purpose of revealing underlying mechanisms) by no means is exclusive.

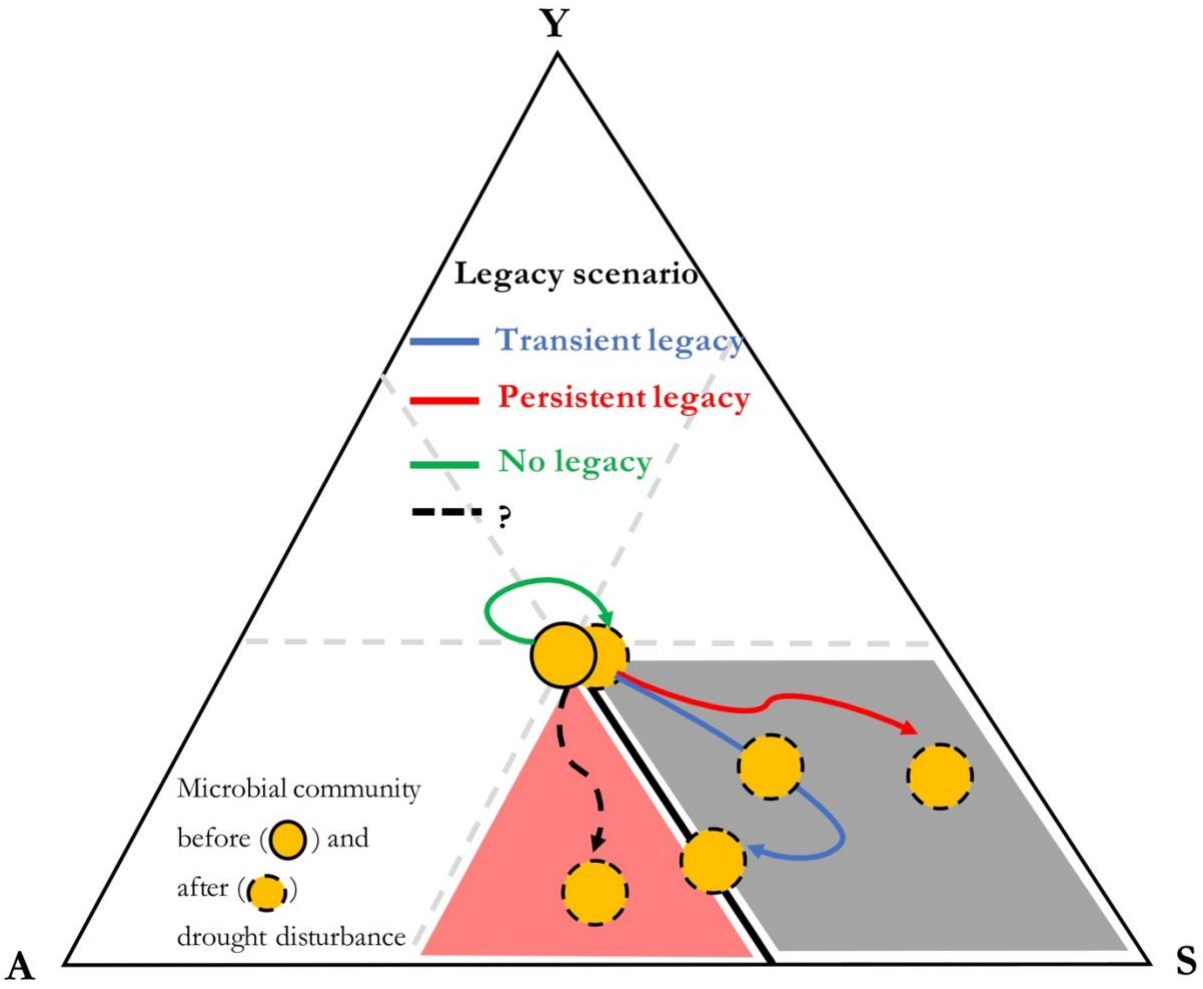

Fig. 5 Coherent organization of drought legacy scenarios into YAS-constrained space. Drought legacy is contingent on the trajectory of a microbial community on the YAS space after drought disturbance. There will be no legacy if a community does not move at all or move along the thick black line. Instead, if the community moves into and stays in the grey region, persistent legacy will occur. However, if the community eventually leaves the grey region and settles on the thick black line, only transient legacy can occur. In addition, a speculation of another trajectory is illustrated: a community moving into the red region with both increased drought tolerance and enzyme investment. Note: it is for an illustration purpose only that the starting microbial community (full yellow circle) does not necessarily stay in the very center of the space.

A coherent mechanistic framework

We can coherently organize the above legacy scenarios with clear contrasts (transient vs. persistent legacy by moderate vs. severe drought disturbance and persistent legacy vs. no legacy by severe drought without vs. with dispersal) into a space constrained by the YAS, as illustrated in **Fig. 5**. Originating from intra-cellular metabolic tradeoff between enzyme and osmolyte production, drought legacy in microbiome functioning is eventually determined by the position that a community can reach on its potential space constrained by enzyme investment, drought tolerance, and yield. Based on this cohesive notion, any factor that affects the trajectory of a community in the YAS strategy space may influence the magnitude and/or duration of a drought legacy. For instance, when drought forces the community to move to a position of higher drought tolerance but eventually similar enzyme investment (e.g., low level drought as shown in the moderate scenario; **Fig. 4A**), a transient legacy occurs. However, when a community moves to a position of higher drought tolerance and lower enzyme investment (e.g., under an intense drought

as shown in the severe scenario; **Fig. 4A**), a persistent legacy with impaired capability in degrading substrates can occur. In contrast, when the community does not shift in strategy space (e.g., with dispersal present; **Fig. 4B**), even transient legacies may not occur.

However, factors and mechanisms influencing the tradeoffs between enzyme investment and drought tolerance can be complex and manifold. In fact, tradeoffs in microbiomes and beyond are complex in general (e.g., **Berezovsky & Shakhnovich 2005; Ferenci 2016**). Notably, a tradeoff is not necessarily rigid; positive relationships between traits may also be observed (e.g., **Tikhonov et al. 2020**). Such complexities could be induced by factors including drought intensity, dispersal, and potentially many others, as well as processes including, e.g., metabolic plasticity and evolution history. For instance, we speculate a fourth legacy scenario of both increased drought tolerance and enzyme investment that emerges from a loss of enzyme-osmolyte tradeoff under certain conditions, which in theory is possible as long as without breaking the constraint of tradeoffs with yield (the red region in **Fig. 5**). Therefore, broadening the scope of scenarios examined in this study (as discussed earlier on drought disturbance and dispersal) and relaxing assumptions in DEMENTpy offer natural directions in which our study can be extended for enriching the tradeoff-mediated mechanisms underpinning drought legacy.

Implications

Our study revealed a tradeoff-mediated mechanistic framework that can explain drought legacies in soil microbiomes emerging from trait-based microbial community shifts. This mechanistic insight has broad consequences for quantifying ecosystems' responses and feedbacks to increasing frequency and severity of drought and other environmental changes. An accurate quantification of drought legacy with respect to magnitude and duration would enable a better

447 evaluation of implications of litter and soil organic matter decomposition for whole ecosystem
448 functioning and dynamics. For instance, even a transient legacy of impaired decomposition of litter
449 may enhance carbon sequestration in soil systems at certain temporal scales, but may also allow
450 fuels to accumulate for the next fire season, thereby increasing fire risk (e.g., **Pellegrini et al.**
451 **2018**). Additionally, impaired decomposition can inhibit release of nutrients from detritus and thus
452 their return to plants, influencing plant-microbe interactions (e.g., **Kaisermann et al. 2017**). All
453 these and potentially many other cascading changes arising from microbiome legacies would
454 engender more complex feedbacks in ecosystems. Evaluating their implications entails an
455 integrative, holistic view of components in systems across ecosystem and the Earth System scales.
456 To proceed, this study clearly indicates that to establish a predictive science of ecosystems in the
457 context of projected global climate change, considering history as an essential component means
458 that dimensions and spaces of essential tradeoffs distilled from tremendous taxonomic diversity
459 should be incorporated. This trait-based modelling of soil microbiome, together with progress in
460 trait-based insights into vegetation dynamics, offer an inspirational starting point for moving
461 forward in this direction.
462
463 **References**
464 Allison, S. D. (2012). A trait-based approach for modelling microbial litter decomposition.
465 Ecology letters, 15, 1058-1070.
466
467 Allison, S. D., & Goulden, M. L. (2017). Consequences of drought tolerance traits for microbial
468 decomposition in the DEMENT model. Soil Biology and Biochemistry, 107, 104-113.
469

Allison, S. D., Lu, Y., Weihe, C., Goulden, M. L., Martiny, A. C., Treseder, K. K., & Martiny, J. B. (2013). Microbial abundance and composition influence litter decomposition response to environmental change. Ecology, 94, 714-725.

Allison, S. D., & Martiny, J. B. (2008). Resistance, resilience, and redundancy in microbial communities. Proceedings of the National Academy of Sciences, 105, 11512-11519.

Amor, D. R., Ratzke, C., & Gore, J. (2020). Transient invaders can induce shifts between alternative stable states of microbial communities. Science Advances, 6, eaay8676.

Anderegg, W. R., Schwalm, C., Biondi, F., Camarero, J. J., Koch, G., Litvak, M., ... & Wolf, A. (2015). Pervasive drought legacies in forest ecosystems and their implications for carbon cycle models. Science, 349, 528-532.

Berdugo, M., Delgado-Baquerizo, M., Soliveres, S., Hernández-Clemente, R., Zhao, Y., Gaitán, J. J., ... & Rillig, M. C. (2020). Global ecosystem thresholds driven by aridity. Science, 367, 787-790.

Berezovsky, I. N., & Shakhnovich, E. I. (2005). Physics and evolution of thermophilic adaptation. Proceedings of the National Academy of Sciences, 102, 12742-12747.

Birch, H. F. 1958. The effect of soil drying on humus decomposition and nitrogen availability. Plant and Soil, 10, 9–31.

Borsa, A. A., Agnew, D. C., & Cayan, D. R. (2014). Ongoing drought-induced uplift in the western United States. Science, 345, 1587-1590.

Conradi, T., Van Meerbeek, K., Ordonez, A., & Svenning, J. C. (2020). Biogeographic historical legacies in the net primary productivity of Northern Hemisphere forests. Ecology Letters, 23, 800-810.

Csonka, L. N. (1989). Physiological and genetic responses of bacteria to osmotic stress. Microbiological Reviews, 53, 121-147.

Cuddington, K. (2011). Legacy Effects: The Persistent Impact of Ecological Interactions. Biological Theory, 6, 203–210.

Evans, S.E., Wallenstein, M.D. (2012) Soil microbial community response to drying and rewetting stress: does historical precipitation regime matter? Biogeochemistry, 109**,** 101–116.

Evans, S. E., & Wallenstein, M. D. (2014). Climate change alters ecological strategies of soil bacteria. Ecology letters, 17, 155-164.

Evans, S. E., Bell-Dereske, L. P., Dougherty, K. M., & Kittredge, H. A. (2020). Dispersal alters soil microbial community response to drought. Environmental Microbiology, 22, 905-916.

516 Falkowski, P. G., Fenchel, T., & Delong, E. F. (2008). The microbial engines that drive Earth's
517 biogeochemical cycles. Science, 320, 1034-1039.
518
519 Ferenci, T. (2016). Trade-off mechanisms shaping the diversity of bacteria. Trends in
520 Microbiology, 24, 209-223.
521
522 Fuchslueger, L., Bahn, M., Hasibeder, R., Kienzl, S., Fritz, K., Schmitt, M., ... & Richter, A. (2016).
523 Drought history affects grassland plant and microbial carbon turnover during and after a
524 subsequent drought event. Journal of Ecology, 104, 1453-1465.
525
526 Fukami, T. (2015). Historical contingency in community assembly: integrating niches, species
527 pools, and priority effects. Annual Review of Ecology, Evolution, and Systematics, 46, 1-23.
528
529 Glassman, S. I., Weihe, C., Li, J., Albright, M. B., Looby, C. I., Martiny, A. C., ... & Martiny, J.
530 B. (2018). Decomposition responses to climate depend on microbial community composition.
531 Proceedings of the National Academy of Sciences, 115, 11994-11999.
532
533 Green, J.K., Seneviratne, S.I., Berg, A.M. *et al.* (2019). Large influence of soil moisture on long-
534 term terrestrial carbon uptake. Nature, 565**,** 476–479.
535
536 Hawkes, C. V., & Keitt, T. H. (2015). Resilience vs. historical contingency in microbial responses
537 to environmental change. Ecology letters, 18, 612-625.
538

539 Hawkes, C. V., Waring, B. G., Rocca, J. D., & Kivlin, S. N. (2017). Historical climate controls
540 soil respiration responses to current soil moisture. Proceedings of the National Academy of
541 Sciences, 114, 6322-6327.
542
543 Herzschuh, U. (2020). Legacy of the Last Glacial on the present-day distribution of deciduous
544 versus evergreen boreal forests. Global Ecology and Biogeography, 29, 198-206
545
546 Hinojosa, M. B., Laudicina, V. A., Parra, A., Albert-Belda, E., & Moreno, J. M. (2019). Drought
547 and its legacy modulate the post-fire recovery of soil functionality and microbial community
548 structure in a Mediterranean shrubland. Global Change Biology, 25, 1409-1427.
549
550 Ives, A. R., & Carpenter, S. R. (2007). Stability and diversity of ecosystems. Science, 317, 58-62.
551
552 Johnstone, J. F., Allen, C. D., Franklin, J. F., Frelich, L. E., Harvey, B. J., Higuera, P. E., ... &
553 Schoennagel, T. (2016). Changing disturbance regimes, ecological memory, and forest resilience.
554 Frontiers in Ecology and the Environment, 14, 369-378.
555
556 Kaisermann, A., de Vries, F. T., Griffiths, R. I., & Bardgett, R. D. (2017). Legacy effects of
557 drought on plant–soil feedbacks and plant–plant interactions. New Phytologist, 215, 1413-1424.
558
559 Karhu, K., Auffret, M., Dungait, J. *et al.* (2014) Temperature sensitivity of soil respiration rates
560 enhanced by microbial community response. Nature, 513, 81–84
561

562 Louca, S., Polz, M.F., Mazel, F. et al. (2018). Function and functional redundancy in microbial
563 systems. Nature Ecology Evolution, 2, 936–943.
564
565 Malik, A.A., Martiny, J.B.H., Brodie, E.L. *et al.* (2020). Defining trait-based microbial strategies
566 with consequences for soil carbon cycling under climate change. ISME J 14, 1–9.
567
568 Manzoni, S., Schimel, J. P., & Porporato, A. (2012). Responses of soil microbial communities to
569 water stress: results from a meta-analysis. Ecology, 93, 930-938.
570
571 Martiny, J., Martiny, A., Weihe, C. et al. (2017). Microbial legacies alter decomposition in
572 response to simulated global change. ISME J 11, 490–499.
573
574 McGill, B. J., Enquist, B. J., Weiher, E., & Westoby, M. (2006). Rebuilding community ecology
575 from functional traits. Trends in Ecology & Evolution, 21, 178-185.
576
577 Meisner, A., Rousk, J., & Bååth, E. (2015). Prolonged drought changes the bacterial growth
578 response to rewetting. Soil Biology and Biochemistry, 88, 314-322.
579
580 Pellegrini, A., Ahlström, A., Hobbie, S. *et al.* (2018). Fire frequency drives decadal changes in soil
581 carbon and nitrogen and ecosystem productivity. Nature, 553**,** 194–198.
582
583 Potts, M. (1994). Desiccation tolerance of prokaryotes. Microbiological Reviews, 58, 755-805.
584

585 Rousk, J., Smith, A. R., & Jones, D. L. (2013). Investigating the long-term legacy of drought and
586 warming on the soil microbial community across five European shrubland ecosystems. Global
587 Change Biology, 19, 3872-3884.
588
589 Schimel, J., Balser, T. C., & Wallenstein, M. (2007). Microbial stress-response physiology and its
590 implications for ecosystem function. Ecology, 88, 1386-1394.
591
592 Staver, A. C., Archibald, S., & Levin, S. A. (2011). The global extent and determinants of savanna
593 and forest as alternative biome states. Science, 334, 230-232.
594
595 Tikhonov, M., Kachru, S., & Fisher, D. S. (2020). A model for the interplay between plastic
596 tradeoffs and evolution in changing environments. Proceedings of the National Academy of
597 Sciences, 117, 8934-8940.
598
599 Tropini, C., Moss, E. L., Merrill, B. D., Ng, K. M., Higginbottom, S. K., Casavant, E. P., ... &
600 Bhatt, A. S. (2018). Transient osmotic perturbation causes long-term alteration to the gut
601 microbiota. Cell, 173, 1742-1754.
602
603 Wang, B., & Allison, S. D. (2019). Emergent properties of organic matter decomposition by soil
604 enzymes. Soil Biology and Biochemistry, 136, 107522.
605
606 Waring, B., Hawkes, C. V. (2018). Ecological mechanisms underlying soil bacterial responses to
607 rainfall along a steep natural precipitation gradient, FEMS Microbiology Ecology, 94, fiy001.

Vila, J. C., Jones, M. L., Patel, M., Bell, T., & Rosindell, J. (2019). Uncovering the rules of microbial community invasions. Nature Ecology & Evolution, 3, 1162-1171.

Wieder, W. R., Allison, S. D., Davidson, E. A., Georgiou, K., Hararuk, O., He, Y., ... & Todd-Brown, K., 2015. Explicitly representing soil microbial processes in Earth system models. Global Biogeochemical Cycles, 29, 1782-1800.

Acknowledgements

All data and code underlying the analyses and illustrations in this manuscript are accessible at: https://github.com/bioatmosphere/microbiome-drought-legacy. DEMENTpy code is available at: https://github.com/bioatmosphere/DEMENTpy.

Supporting Information

Tradeoff-mediated Drought Legacy in Soil Microbiome

Bin Wang, Steven D. Allison

1 DEMENTpy

DEMENTpy, a trait-based explicit microbial systems modelling framework both mechanistically and spatially, is an effort of mechanistically updating (see **Supporting Fig. 1** for conceptual structure) and programmatically restructuring (see **Supporting Fig. 7** for programming structure) DEMENT that was initially developed in 2012 (**Allison 2012**). The source code in Python is accessible at https://github.com/bioatmosphere/DEMENTpy. Processes simulated in DEMENTpy are described below.

1.1 Microbial community initialization

With a trait-based approach, a microbial pool comprises a large number of hypothetical taxa in DEMENTpy is created by randomly drawing values from distributions of various microbial and enzymatic traits (**Supporting Table 1**) and assigning them to different taxa. These hypothetical taxa in the microbial pool with differing combinations of trait values are randomly placed on the spatial grid to form a spatially-explicit microbial community. See animations at https://bioatmosphere.github.io/DEMENTpy/ to get an intuitive notion of this spatial feature, and an application of this feature to addressing enzymatic heterogeneity scaling in **Wang and Allison (2019)**. Trait distributions are all assumed to follow uniform distributions, except that for simplicity, some traits are assumed to be constants, and values of some traits are derived from established correlations with other traits. These distributions and assumptions are largely informed by field- and lab-based experimental works (**Allison 2012; Allison and Goulden 2017**).

Four of the major traits determining intra-cellular metabolism of enzyme and osmolyte and thus mass balance are rates of enzyme production (constitutive and inducible) and rates of osmolyte production (constitutive and inducible). On top of these rates, taxon-specific number of genes encoding different enzymes and osmolytes are determined randomly under the constraint of systems setup. Therefore, rate and number together determine the amounts of enzyme and osmolyte a cell can produce. The rate of inducible osmolyte production is then normalized to a value from 0 to 1, which is regarded as drought tolerance. Such a treatment of drought tolerance is an update to the previous version which instead directly introduced a drought tolerance parameter and imposed a penalty on carbon use efficiency accordingly (**Allison and Goulden 2017**). Starting from osmolyte production to determine drought tolerance is supposed to be more biologically realistic (**Schimel 2007**). Additionally, a whole set of enzymatic traits including Vmax and Km of both enzyme and transporter are employed to explicitly parameterize a certain number of different enzymes and transporters allowed in a system.

1.2 Metabolic production of enzyme and osmolyte

Different individuals (hypothetical taxa) comprising the microbial community complete their demographic processes of growth, mortality, and reproduction while degrading substrates and ingesting monomers under the influence of temperature and water potential. From these underlying processes emerges dynamics and functioning at both the microbial cell level and the whole system level.

Degradation of substrates are calculated explicitly by using different enzymes with different kinetic properties. One principle during the simulation is that every substrate at least has one enzyme to degrade and vice versa. Monomers' uptake is calculated explicitly by having differing transporters to target them; transporters of different types and amounts are taxon-specific.

The governing equation of both substrates' degradation and monomers' uptake follows the Michaelis-Menten equation, which is constrained by temperature (accounting for temperature impacts on enzymatic kinetics) and water potential (accounting for enzymatic kinetics and diffusion declines arising from drought; **Allison and Goulden 2017**):

$$V = \frac{V_{max} f(T)[S][E]}{K_m + [S]} f(\psi)$$

$$f(T) = e^{\left(-\frac{\boldsymbol{\varepsilon}}{R}\left(\frac{1}{T} - \frac{1}{T_{ref}}\right)\right)}$$

$$f(\psi) = e^{k\psi}$$

where *E* and *S* are matrices and represent enzyme and substrate concentration, respectively, *Vmax* represents the enzyme catalytic constant, K_m denotes the concentration of *S* at which *V* is one half V_{max}, $\boldsymbol{\varepsilon}$ is enzymatic activation energy, *R* is universal gas constant, and *k* is a coefficient controlling water potential sensitivity that distinguishes between degradation and uptake.

Intra-cellular production of enzymes and osmolytes are described below in detail with respect to simulation methods and their underlying rationales. Cellular metabolism explicitly deals with both the carbon upon uptake from degraded substrates and the biomass carbon of microbial cells inducibly and constitutively (**Supporting Fig. 3**). The metabolic processing of assimilated carbon after growth respiration (constrained by a constant) is directed to enzyme (and respiration) and osmolyte production (and respiration), which are treated horizontally in the model without prescribing an order. The carbon left after these processes accumulates toward biomass. We assume the constitutive osmolyte production rate (*Osmo_Con*) varies across taxa independent of water potential, accounting for bacterial/fungal cell's allocation of biomass to keep a water potential balance across cell wall (**Csonka 1989; Potts 1994**). In contrast, taxon-specific inducible

production of osmolytes (O_{ind}) is subject to constraint from water potential and is calculated following:

$$O_{ind}(i) = \begin{cases} O_{ind}(i), & \psi \geq \psi_{th} \\ O_{ind}(i)\ (1\ -\ \alpha\psi), & \psi < \psi_{th} \end{cases}$$

where O_{ind}, indexed by taxon i, is the i_{th} taxon's inducible osmolyte production rate, ψ is the daily water potential, α is a water potential coefficient determining water potential sensitivity, and ψ_{th} is a system water potential constant, below which inducible osmolyte production is activated. Though with a differing production rate across taxa, osmolyte in the current version (without further differentiating among different osmolytic compounds) is assumed to hold a constant stoichiometry of C/N = 3, which governs consumption of N in intracellular metabolism. This ratio is based on an average of the three most common osmotic compounds in bacteria (**Csonka 1989; Potts 1994**): proline ($C_5H_9NO_2$), glycine betaine ($C_5H_{11}NO_2$), and glutamine ($C_5H_{10}N_2O_3$).

Arising from metabolic production of enzyme and osmolyte, mortality of microbial cells is simulated both deterministically by accounting for mass balance relative to a threshold and stochastically based on death probability constrained by drought tolerance and water potential. Here the taxon-specific mortality probability (*Mort*) is calculated following:

$$Mort_i = Death\_basal_i[1 - Death\_rate_i(1 - Tol_i)(\psi - \psi_{th})\ ]$$

where *Death_basal*, indexed by *i*, is the i_{th} taxon's basal mortality probability, *Death_rate* is a death probability coefficient controlling water potential sensitivity, *Tol* is i_{th} taxon's drought tolerance, and ψ_{th} is a system water potential constant. Microbial cells that are either out of mass

balance or randomly killed are designated as dead ones, removed from the microbial community, and added into the substrate pools as dead microbes. Microbial reproduction is simply calculated by splitting microbes into two halves, which disperse to surrounding grid boxes on the spatial grid (**Allison 2012**).

2. Calculation of community-level traits

Community-level enzyme investment (E_{com}) and drought tolerance (D_{com}) weighted by biomass are calculated as:

$$E_{com} = \sum_{i}^{n} EiMi$$

$$D_{com} = \sum_{i}^{n} DiMi$$

respectively, where *Ei* and *Di* refer to the ith taxon's enzyme production rate and drought tolerance, respectively, and *Mi* is the relative biomass of the i_{th} taxon in the community.

References

Allison, S. D. (2012). A trait-based approach for modelling microbial litter decomposition. Ecology letters, 15, 1058-1070.

Allison, S. D., & Goulden, M. L. (2017). Consequences of drought tolerance traits for microbial decomposition in the DEMENT model. Soil Biology and Biochemistry, 107, 104-113.

Bugmann, H., Fischlin, A., & Kienast, F. (1996). Model convergence and state variable update in forest gap models. Ecological Modelling, 89, 197-208.

Csonka, L. N. (1989). Physiological and genetic responses of bacteria to osmotic stress. Microbiological Reviews, 53, 121-147.

Potts, M. (1994). Desiccation tolerance of prokaryotes. Microbiological Reviews, 58, 755-805.

Schimel, J., Balser, T. C., & Wallenstein, M. (2007). Microbial stress-response physiology and its implications for ecosystem function. Ecology, 88, 1386-1394.

Wang, B., & Allison, S. D. (2019). Emergent properties of organic matter decomposition by soil enzymes. Soil Biology and Biochemistry, 136, 107522.

Supporting Table 1 Major microbial and enzyme parameters and their values

Parameter	Value	Unit	Note
max_size_b	2	mg cm-3	C quota threshold for bacterial cell division
Cfrac_b	0.825	mg mg-1	Bacterial C fraction
Nfrac_b	0.16	mg mg-1	Bacterial N fraction
Pfrac_b	0.015	mg mg-1	Bacterial P fraction
Crange	0.09	mg mg-1	Tolerance on C fraction
Nrange	0.04	mg mg-1	Tolerance on N fraction
Prange	0.005	mg mg-1	Tolerance on P fraction
C_min	0.086	mg cm-3	threshold C concentration for cell death
N_min	0.012	mg cm-3	threshold P concentration for cell death
P_min	0.002	mg cm-3	threshold C concentration for cell death
Uptake_C_cost_min	0.01	transporter mg-1 biomass C	Minimun per enzyme C cost as a fraction of uptake
Uptake_C_cost_max	0.1	transporter mg-1 biomass C	Maximum per enzyme C cost as a fraction of uptake
Uptake_Maint_cost	0.01	mg C transporter-1 day-1	Respiration cost of uptake transporters
Enz_per_taxon_min	0		Minimum number of enzymes a taxon can produce
Enz_per_taxon_max	40		Maximum number of enzymes a taxon can produce
Enz_Prod_min	0.00001	mg C mg-1 day-1	Minimum per enzyme production cost as a fraction of C uptake rate
Enz_Prod_max	0.0001	mg C mg-1 day-1	Maximum per enzyme producton cost as a fraction of C uptakte rate
Constit_Prod_min	0.00001	mg C mg-1 day-1	Minimum per enzyme production cost as a fraction of biomass C
Constit_Prod_max	0.0001	mg C mg-1 day-1	Maximum per enzyme production cost as a fraction of biomass C
Osmo_per_taxon_min	1		Minimum number of osmolyte a taxon can produce
Osmo_per_taxon_max	1		Maximum number of osmolyte a taxon can produce
Osmo_Consti_Prod_min	0.0000001	mg C mg-1 day-1	Minimum per osmolyte production cost as a fraction of biomass C
Osmo_Consti_Prod_max	0.000001	mg C mg-1 day-1	Maximum per osmolyte production cost as a fraction of biomass C
Osmo_Induci_Prod_min	0.01	mg C mg-1 day-1	Minimum per osmolyte production cost as a fraction of C uptake rate
Osmo_Induci_Prod_max	0.1	mg C mg-1 day-1	Maximum per osmolyte production cost as a fraction of C uptake rate
CUE_ref	0.5	mg mg-1	Growth efficiency at the reference temperature
CUE_temp	-0.005	mg mg-1	Growth efficiency change with enzyme investment
death_rate_bac	0.001		Bacterial death rate
basal_bac	10		Bacterial basal death probability
wp_th	-2		water potential threshold at which osmolyte is induced
alpha	0.01		Osmolyte production change with water potential
Vmax0_min	5	mg substrate mg-1 enzyme day-1	Minimum Vmax for enzyme
Vmax0_max	50	mg substrate mg-1 enzyme day-1	Maximum Vmax for enzyme

Uptake_Vmax0_min	1	mg substrate mg-1 substrate day-1	Minimum uptake Vmax
Uptake_Vmax0_max	10	mg substrate mg-1 substrate day-1	Maximum uptake Vmax
Uptake_Ea_min	35	kj mol-1	Minimum activation energy for uptake
Uptake_Ea_max	35	kj mol-1	Maximum activation energy for uptake
Km_min	0.01	mg cm-3	Minimum Km
Uptake_Km_min	0.001	mg cm-3	Minimum uptake Km
Vmax_Km	1	mg enzyme day cm-3	Slope for Km-Vmax relationship
Vmax_Km_int	0	mg cm-3	Intercept for Km-Vmax relationship
Uptake_Vmax_Km	0.2	mg biomass day cm-3	Slope for uptake Km-Vmax relationship
Uptake_Vmax_Km_int	0	mg cm-3	Intercept for uptake Km-Vmax relationship
Specif_factor	1		Efficiency-specificity

125

Supporting Table 2 Substrate concentrations initialized in DEMENT simulations (mg cm^{-3}).

Substrate	C	N	P
DeadMic	0	0	0
DeadEnz	0	0	0
Cellulose	146.89	0	0
Hemicellulose	85.855	0	0
Starch	12.21	0	0
Chitin	4.9952	0.83254	0
Lignin	48.51	0.40425	0
Protein1	10.6	2.09704	0
Protein2	10.6	2.09704	0
Protein3	10.6	2.09704	0
OrgP1	12.48	0	0.478469
OrgP2	1.8182	0.79745	0.478469

126

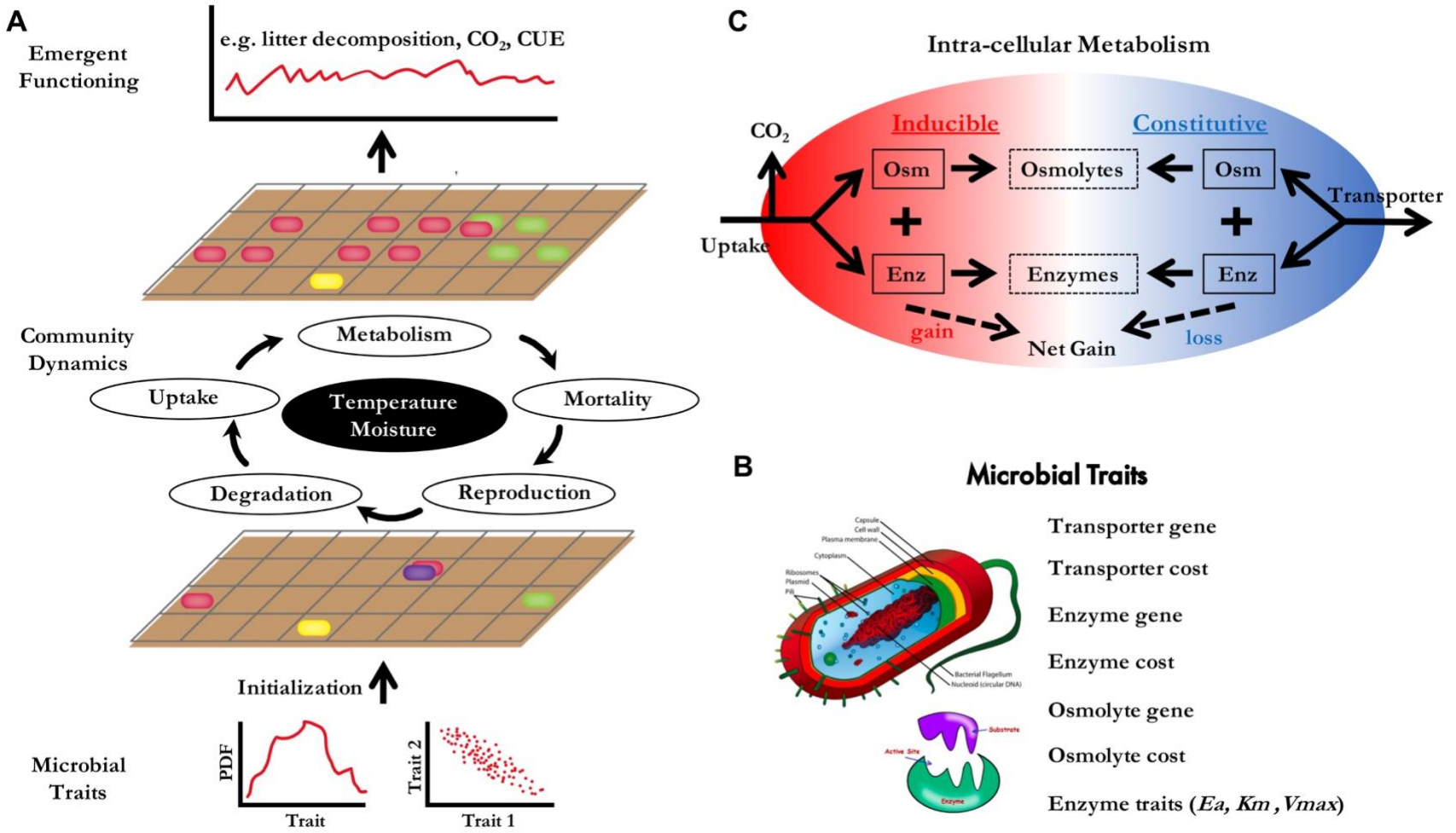

Supporting Fig. 1 DEMENTpy conceptual structure (A) and underpinning traits (B) and intra-cellular metabolisms (C).

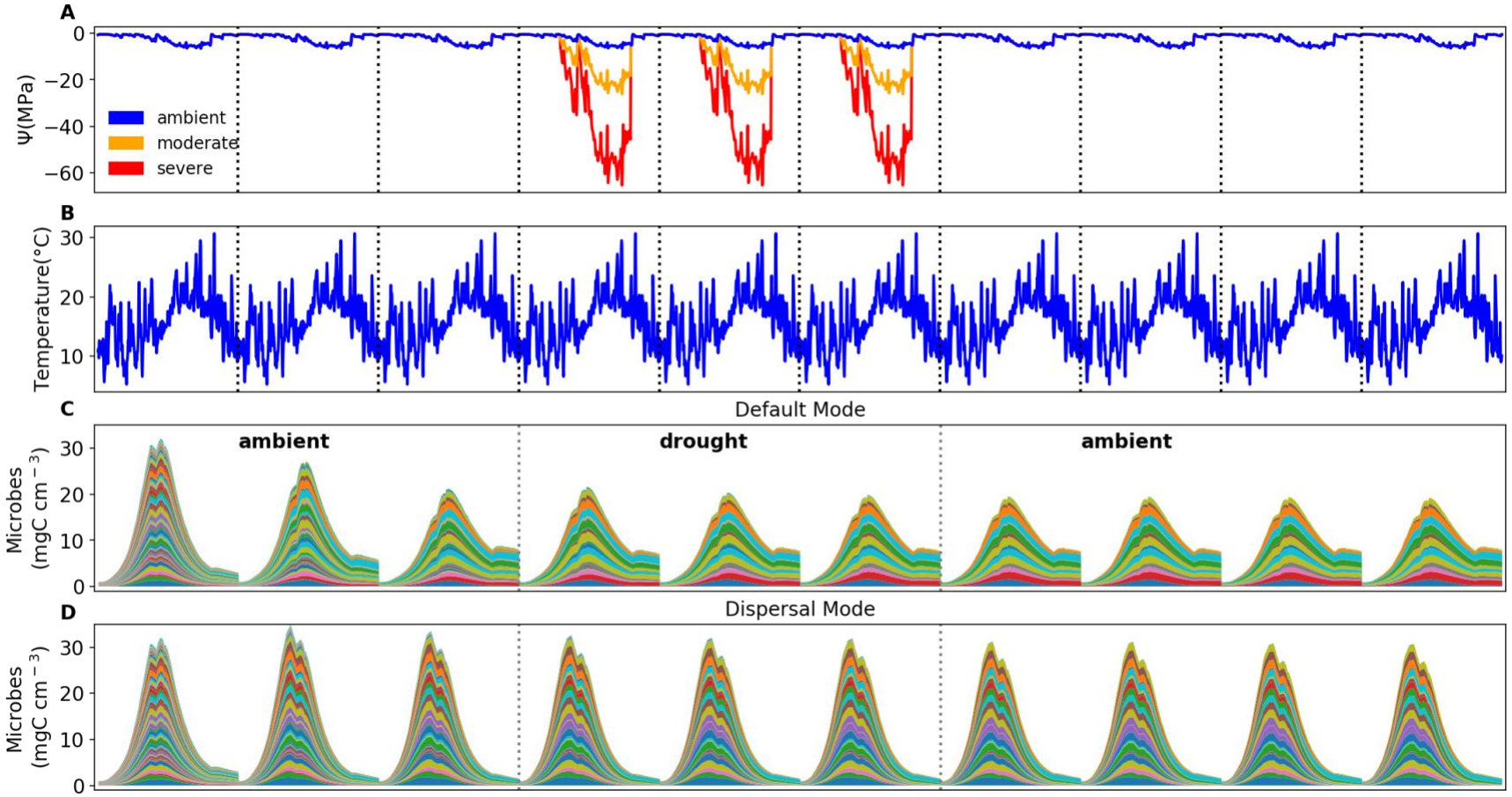

Supporting Fig. 2 Environmental forcing and microbial community dynamics. (**A**) Ambient daily water potential of 2011, with the orange and red line denoting the moderate and severe drought scenario, respectively, which are manipulated values simply by multiplying the water potential across the dry season (from April through September) by 4 and 10, respectively. (**B**) The corresponding daily temperature in 2011. (**C, D**) Microbial community dynamics of the default vs. dispersal mode over 10 years under the ambient

drought scenario. The simulation comprises three phases as separated by the dashed grey lines: a spin-up phase of three years to realize a relatively stable community; a disturbance phase of imposing different drought scenarios for three years; and a final recovery phase after drought disturbance for four years. Colored bands represent different hypothetical taxa in biomass.

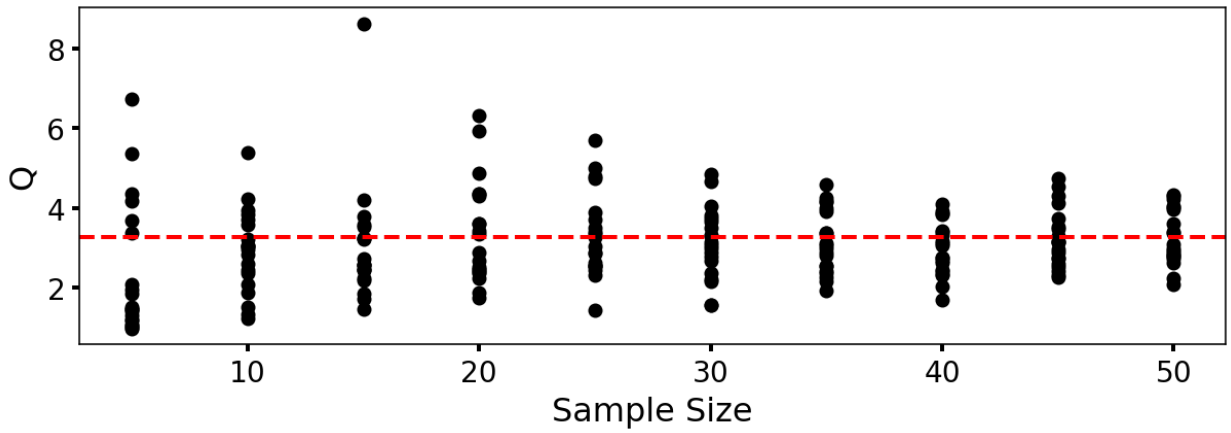

Supporting Fig. 3 DEMENTpy (v1.0) stochasticity convergence analysis. Q (quotient) is calculated as (90% percentile -10% percentile)/median with the data of degradation of substrates following Bugmann et al. (1996). Each sample size has 20 replicates that were randomly drawn from a sample pool of 112 runs. This analysis illustrates that a sample size (i.e., ensemble of simulations) of 40, which starts displaying relatively stabilized and converged variation, may be an appropriate choice considering a tradeoff of reliability vs. consumption of computing resource.

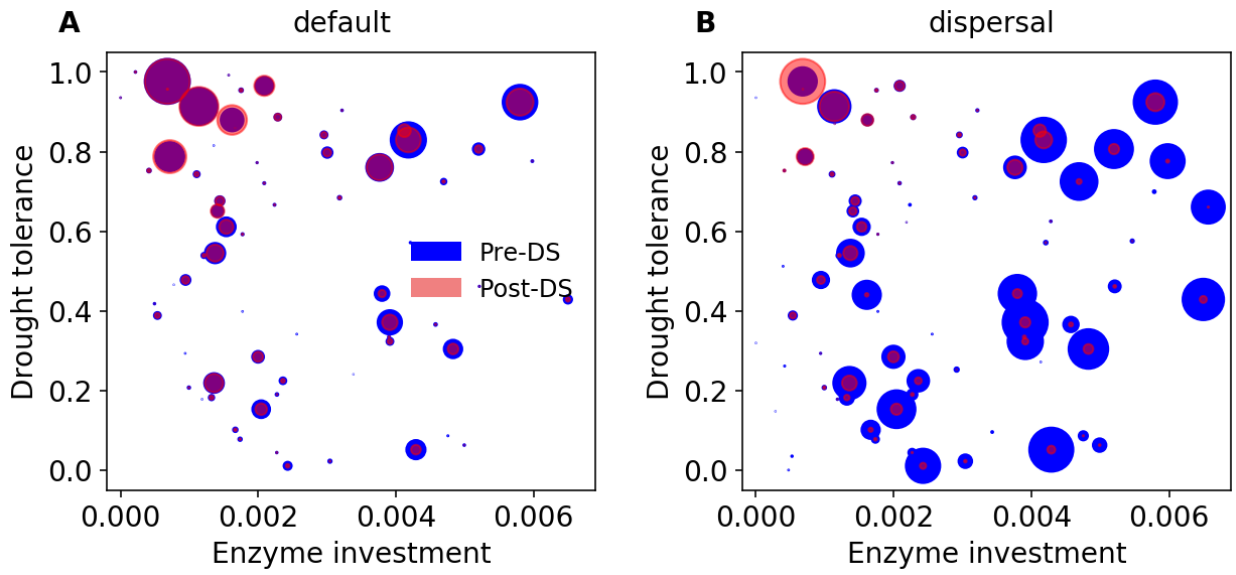

144

145 **Supporting Fig. 4 Taxonomic changes in traits across dry season. (A)** Taxon-specific traits of
146 drought tolerance and enzyme investment of a microbial community without dispersal before (blue)
147 and after the dry season (red) under the ambient scenario. (**B**) The same for a microbial community
148 with dispersal. Each point corresponds to a different taxon, and the size is proportional to its
149 biomass.

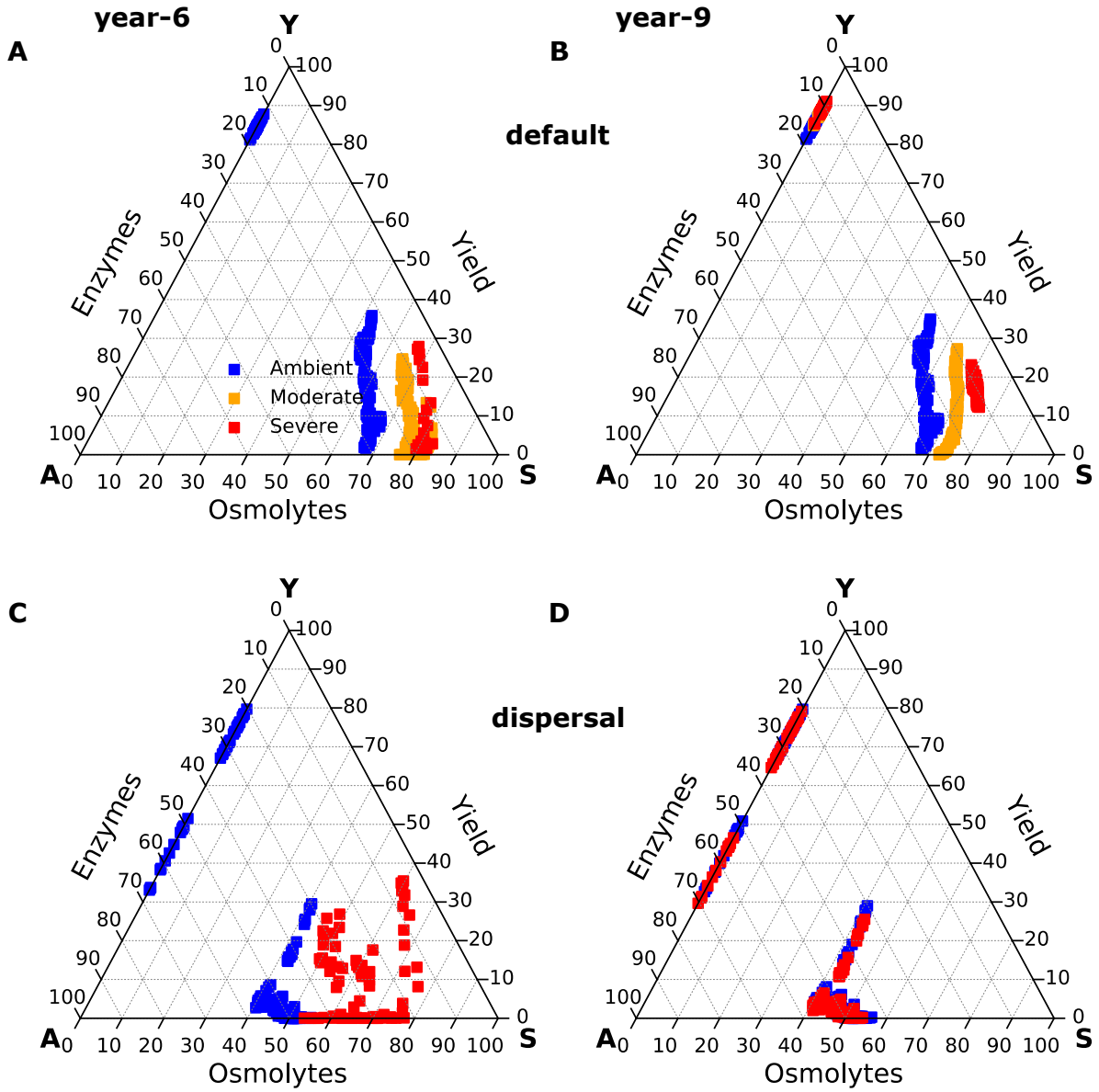

150

151 **Supporting Fig. 5 Ternary plots of community-level allocation of assimilated carbon among**
152 **enzymes, osmolytes, and yield over time under different drought scenarios. (A, B)** Enzyme-
153 Osmolyte-Yield tradeoff of communities during year 6 (3rd year under drought) and year 9 (3rd
154 year after drought), respectively, of the default mode (without dispersal). **(C, D)** The same for the
155 dispersal mode. The Y (Yield), A (Acquisition), and S (Stress) labeled at corners correspond to
156 yield, enzymes, and osmolytes, respectively. Points with negative net biomass gain were omitted.

157

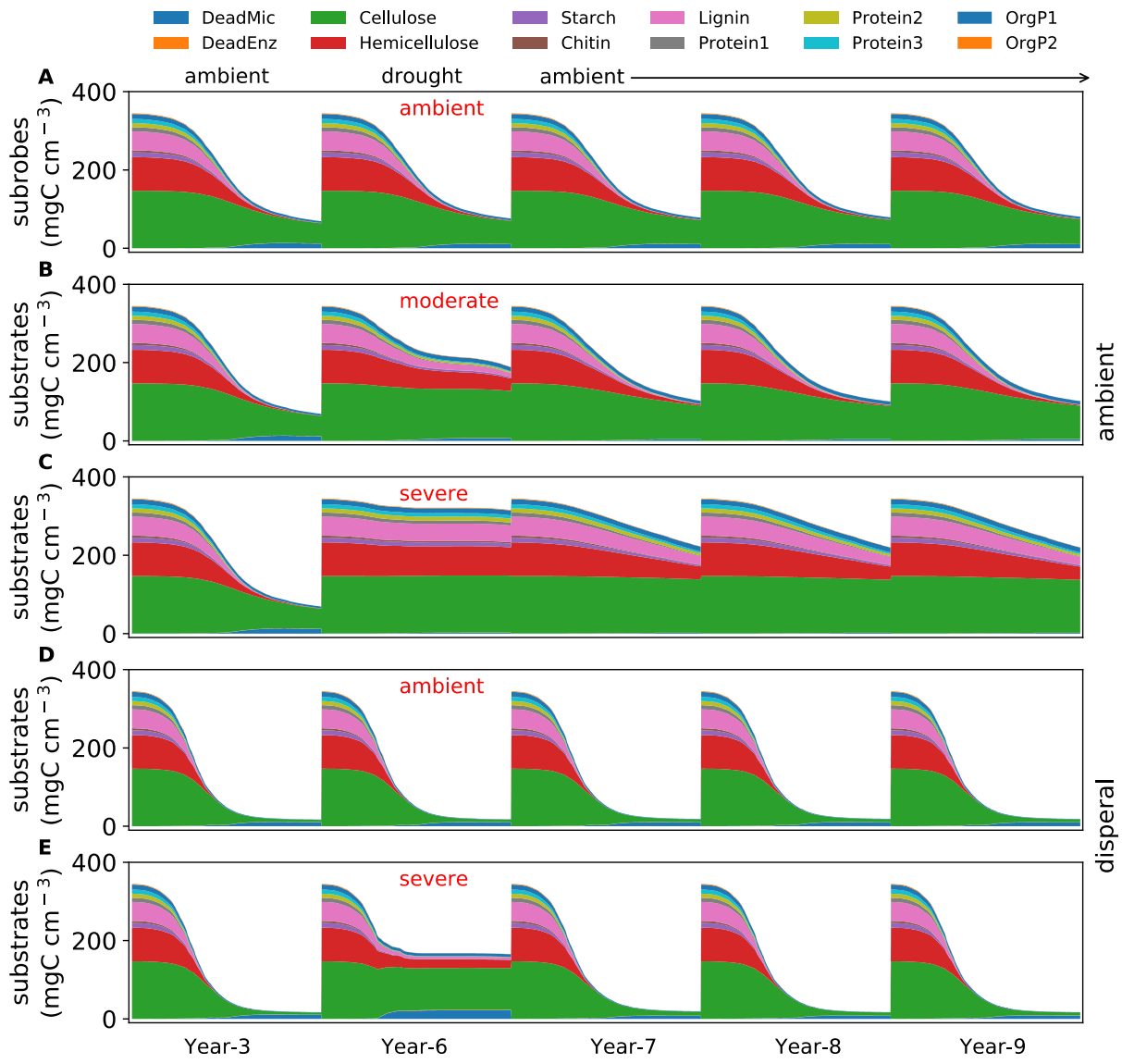

158

159 **Supporting Fig. 6 Substrate-specific dynamics under differing drought scenarios. (A, B, C)**

160 the dynamics under ambient, moderate, and severe scenarios in default mode for year 3 and year

161 6 (the 3rd year under drought disturbance) through year 9. (**D, E**) The same for the dispersal mode

162 but with only ambient and severe scenarios. Each color band represents one type of 12 different

163 substrates.

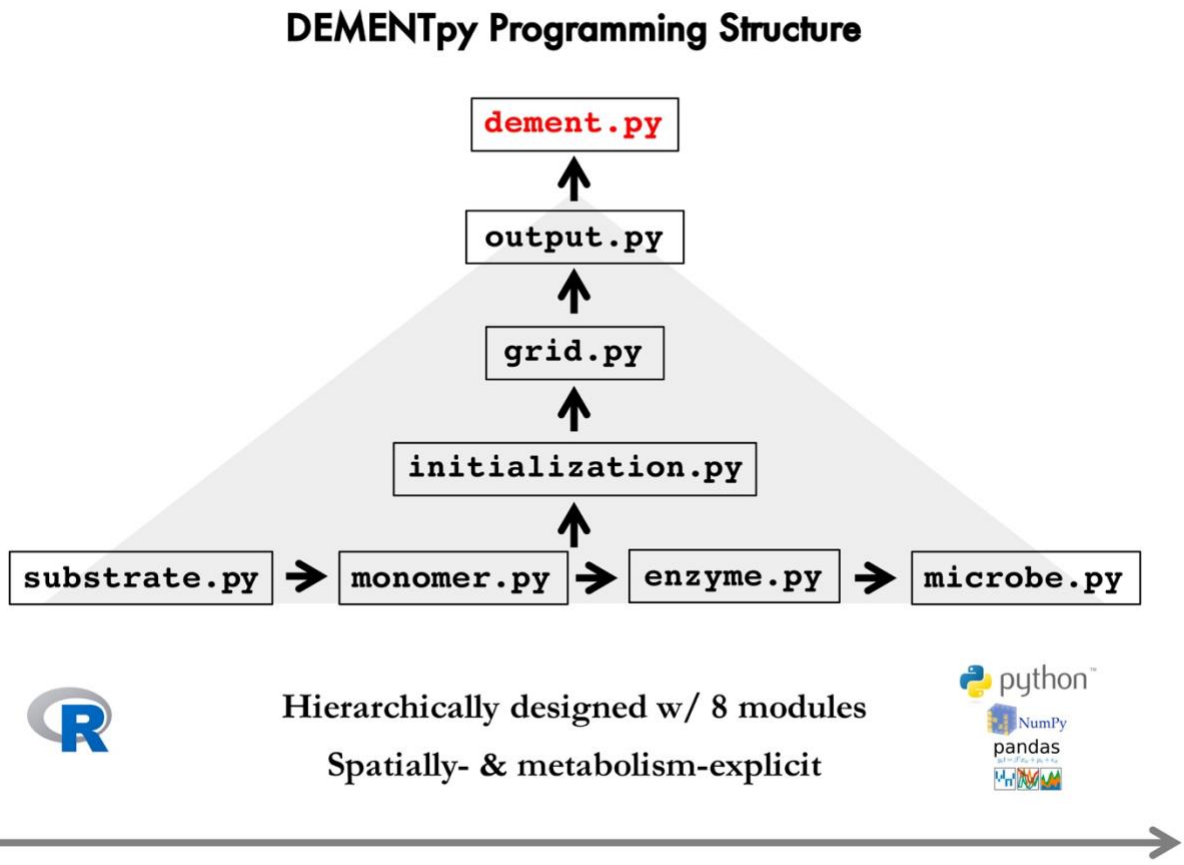

164

165 **Supporting Fig. 7 DEMENTpy programming structure.** DEMENTpy emerges from

166 hierarchically restructuring and mechanistically updating DEMENT programmed in R.